



华南师范大学
SOUTH CHINA NORMAL UNIVERSITY



J/ψ R_{AA} in Au + Au collisions at $\sqrt{s_{NN}} = 14.6, 17.3, 19.6$ and 27GeV

Wei Zhang

South China Normal University



STAR

- Motivation
- J/ψ Suppression Measurements
 - Raw Signal Extraction
 - pp Baseline
 - R_{AA} Results
- Summary

Introduction



➤ Quarkonia suppression was proposed as a sensitive probe to QGP properties

- Dominantly produced before QGP formation

➤ **Hot medium effects**

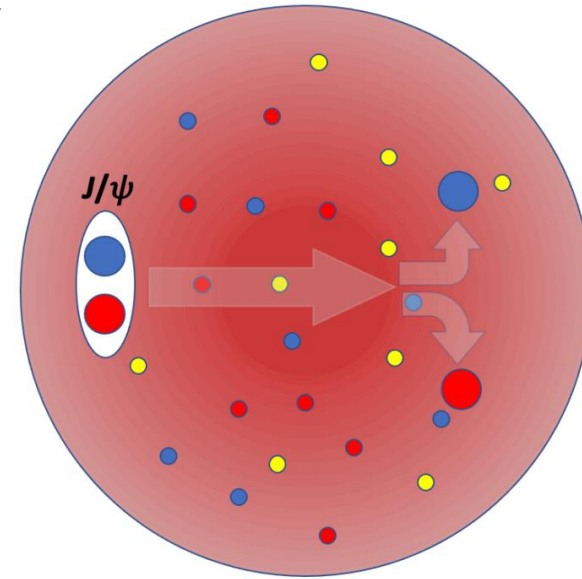
- Dissociation(color screening and dynamic interaction)
- Regeneration

➤ **Cold nuclear matter effects**

- nPDF
- Nuclear absorption

➤ **Other effects**

- Comover interactions
- Feed-down contribution



Credit: Q. Yang

$$R_{AA} = \frac{\sigma_{\text{inel}}}{\langle N_{\text{coll}} \rangle} \frac{d^2 N_{AA} / dy dp_T}{d^2 \sigma_{pp} / dy dp_T}$$

Introduction



➤ Quarkonia suppression was proposed as a sensitive probe to QGP properties

- Dominantly produced before QGP formation

➤ **Hot medium effects**

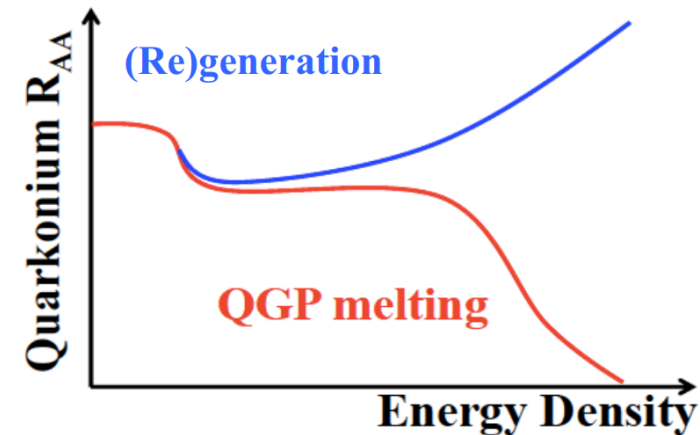
- Dissociation(color screening and dynamic interaction)
- Regeneration

➤ **Cold nuclear matter effects**

- nPDF
- Nuclear absorption

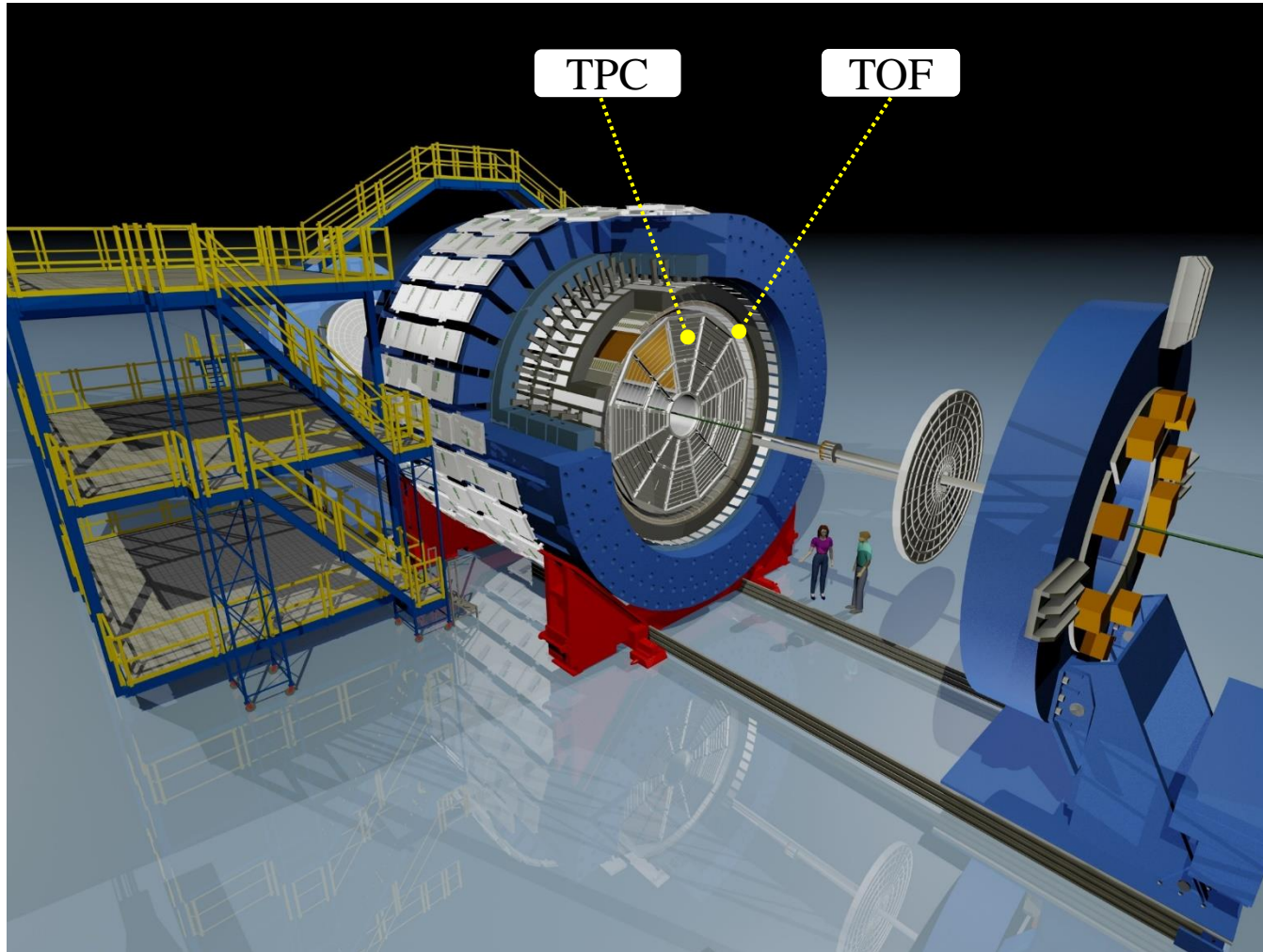
➤ **Other effects**

- Comover interactions
- Feed-down contribution



$$R_{AA} = \frac{\sigma_{\text{inel}}}{\langle N_{\text{coll}} \rangle} \frac{d^2 N_{AA} / dy dp_T}{d^2 \sigma_{pp} / dy dp_T}$$

STAR Detector



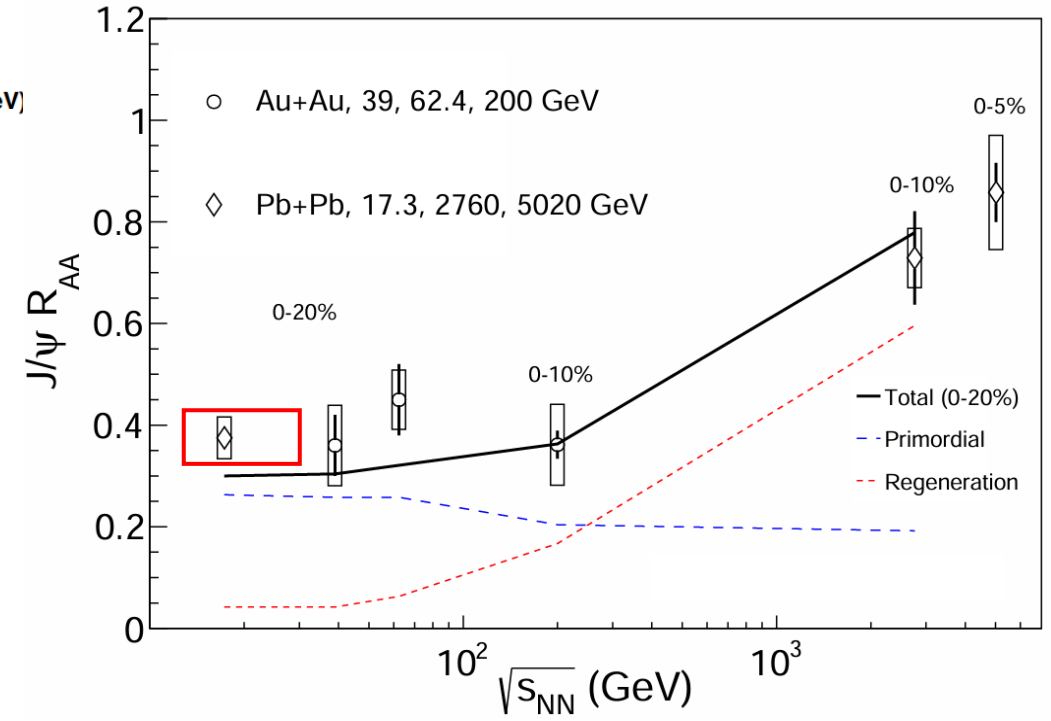
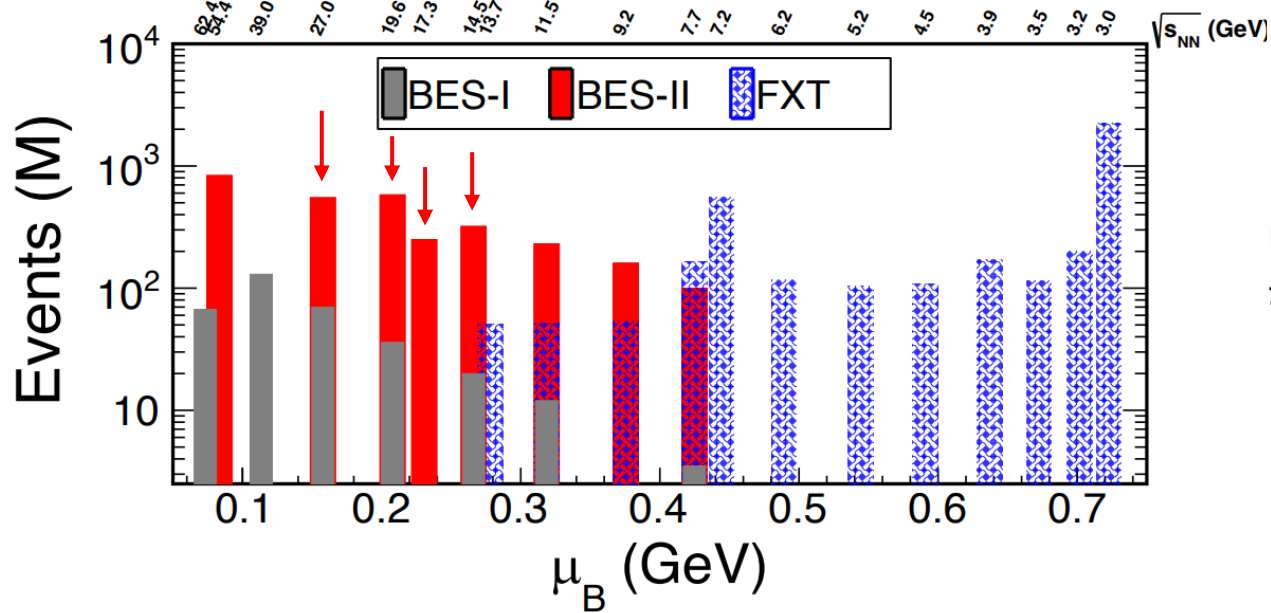
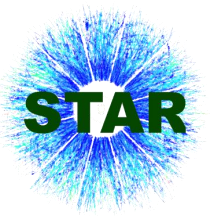
➤ Time Projection Chamber

- Tracking
- Momentum and energy loss
- Acceptance: $|\eta| < 1.5$; $0 \leq \varphi < 2\pi$

➤ Time Of Flight Detector

- Time of flight
- Particle identification
- Acceptance: $|\eta| < 1$; $0 \leq \varphi < 2\pi$

Au+Au Collisions at STAR



STAR Collaboration *Phys. Lett. B* 771 (2017) 13–20

➤ BES-I → BES-II

- 10-20 times higher statistics than BES-I
- Enables differential measurements at low collision energies

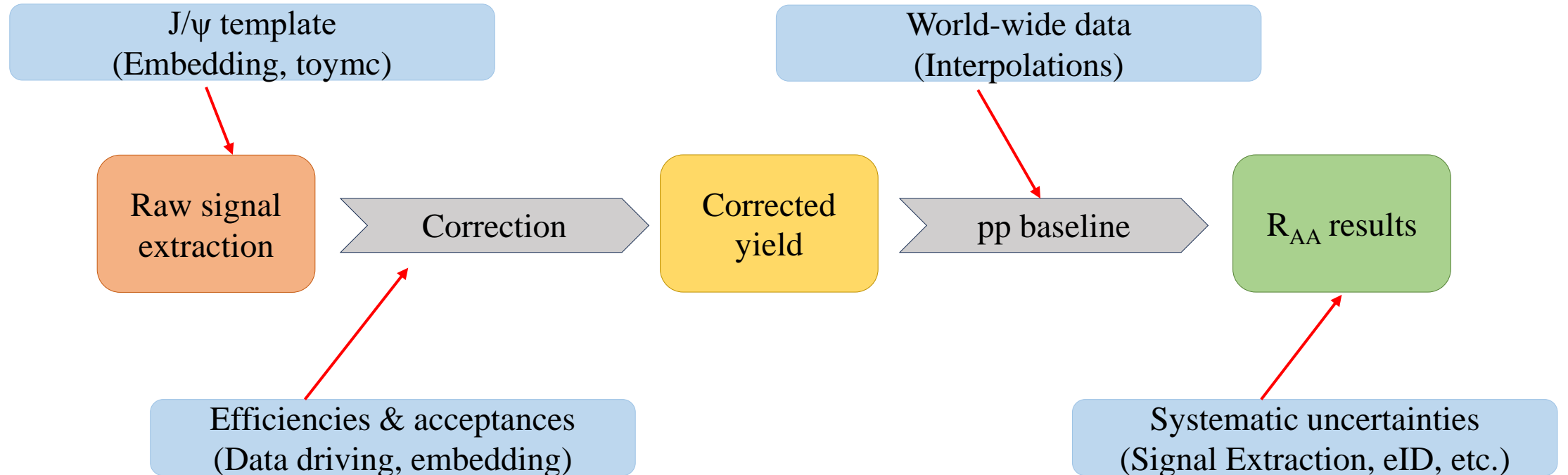
➤ Collision energy dependence of J/ψ production

- Au+Au collisions at $\sqrt{s_{NN}} = 14.6, 17.3, 19.6, 27$ GeV
- Smaller regeneration effect

Analysis Procedure



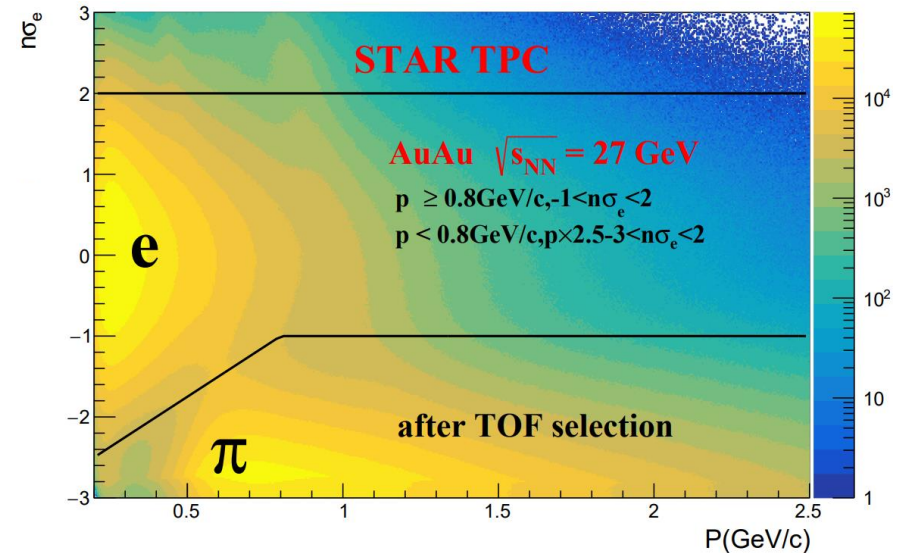
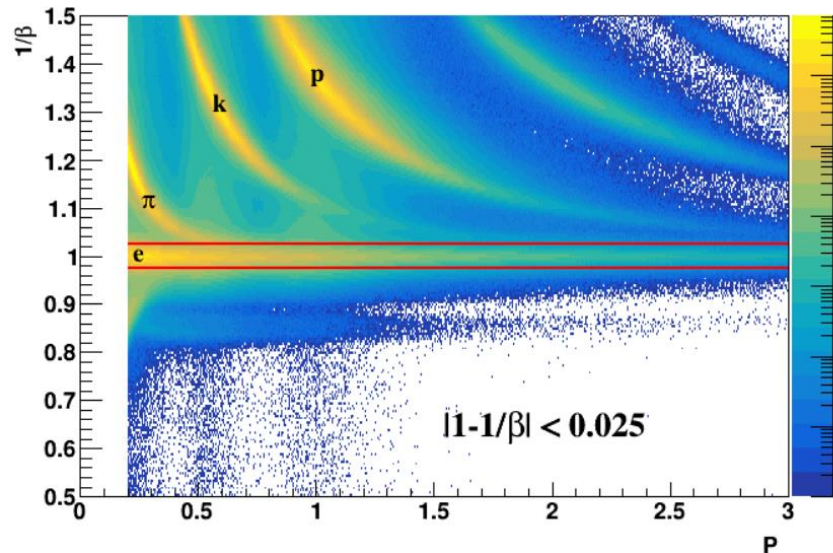
Observable: $R_{AA} = \frac{\sigma_{\text{inel}}}{\langle N_{\text{coll}} \rangle} \frac{d^2 N_{AA}/dydp_T}{d^2 \sigma_{pp}/dydp_T}$ $\left\{ \begin{array}{l} < 1 \text{ suppression} \\ = 1 \text{ no net medium effects} \\ > 1 \text{ enhancement} \end{array} \right.$



Electron Identification

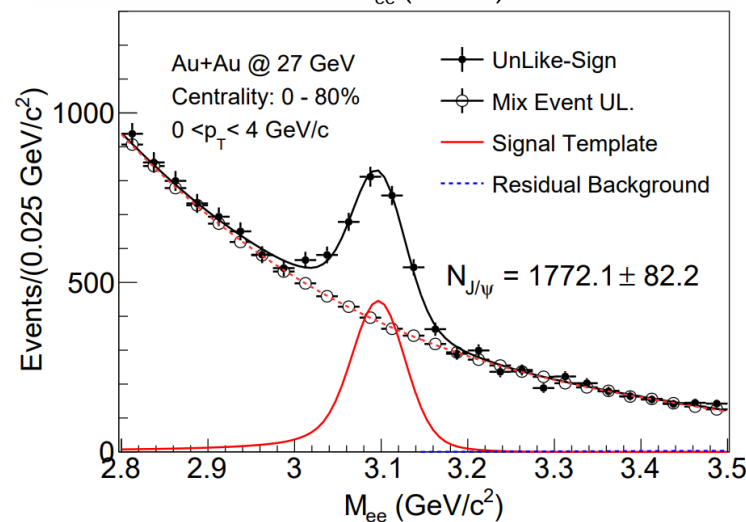
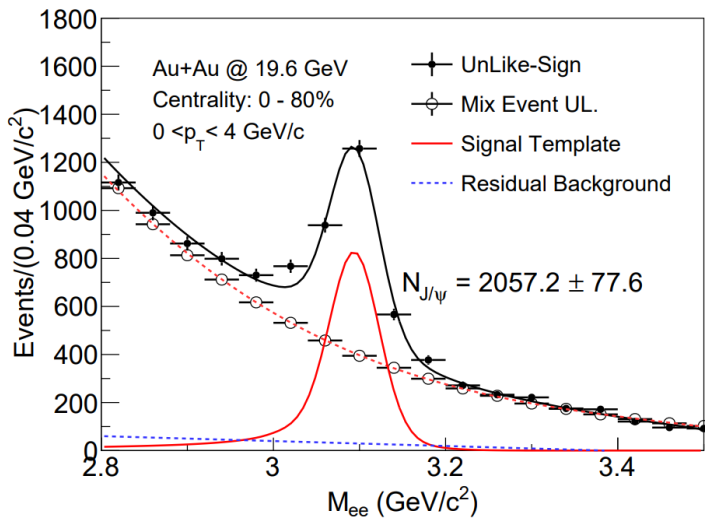
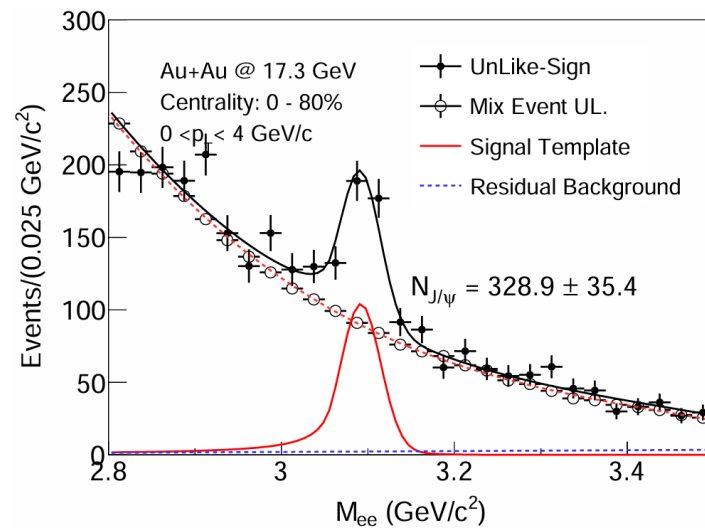
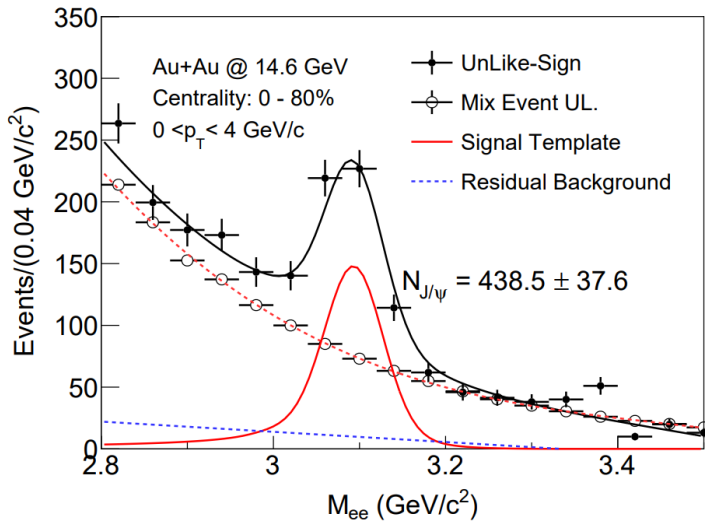
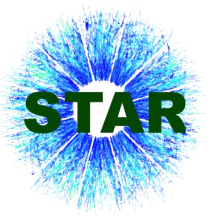


- System : Au+Au collisions in RHIC-STAR
- Collision Energy: 14.6, 17.3, 19.6, 27 GeV
- Decay Channel: $J/\psi \rightarrow e^- + e^+$



$$n\sigma_e = \frac{1}{R} \log \frac{(dE/dx)_{measured}}{(dE/dx)_{electron}}$$

Raw J/ψ Signal



➤ Fitting components include:

- J/ψ template(simulation)
- combinatorial background(mixed event)
- residual background(straight line)

Efficiency and Acceptance Corrections

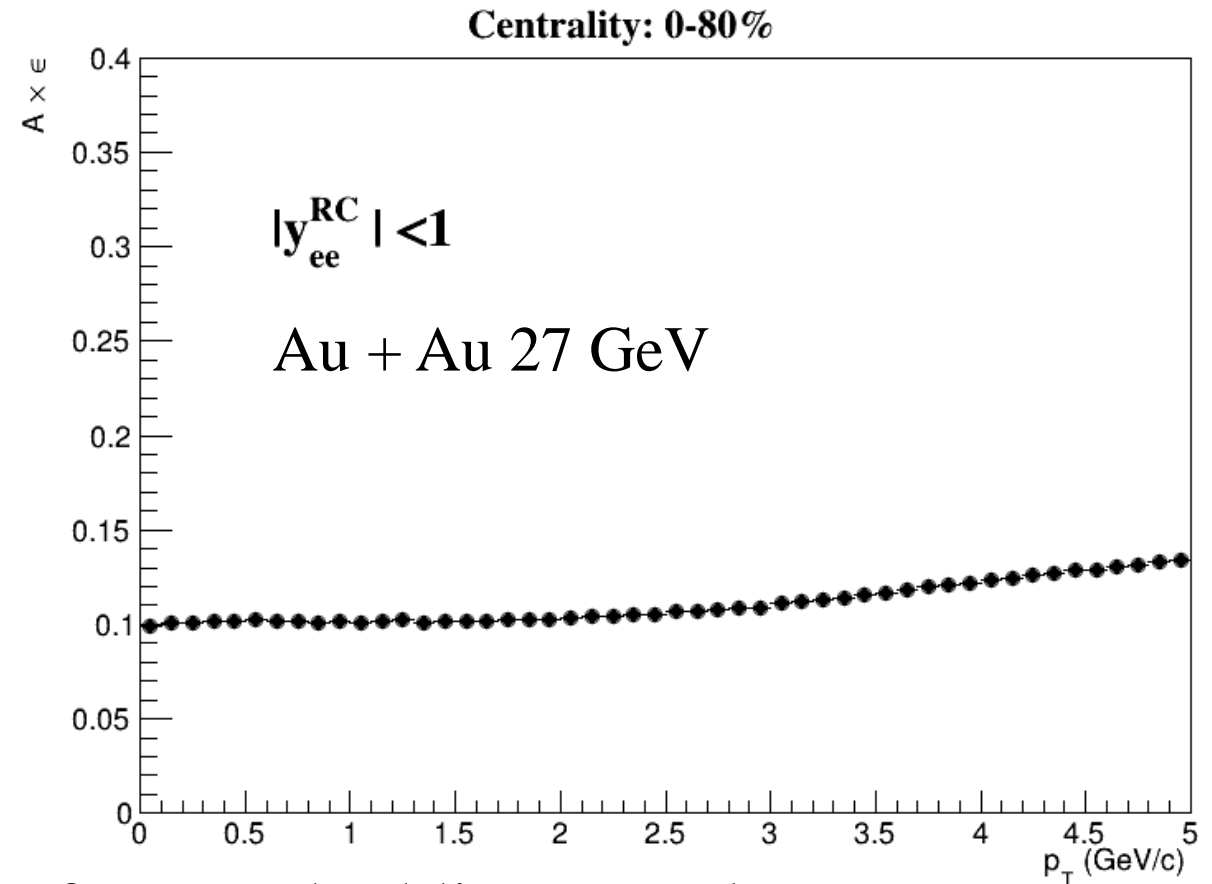


$$R_{AA} = \frac{\sigma_{\text{inel}}}{\langle N_{\text{coll}} \rangle} \frac{d^2 N_{AA} / dy dp_T}{d^2 \sigma_{pp} / dy dp_T}$$

$$N_{AA} = \frac{N_{J/\psi \rightarrow e^+e^-}}{A \times \epsilon \times N_{\text{even}_t}}$$

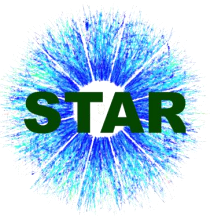
$$\epsilon = \epsilon_{\text{electron}} \times \epsilon_{\text{positron}}$$

$$\epsilon_{\text{electron}} = \epsilon_{\text{positron}} = \epsilon_{\text{TPC}} \times \epsilon_{\text{eID}} \times \epsilon_{\text{TOF}}$$

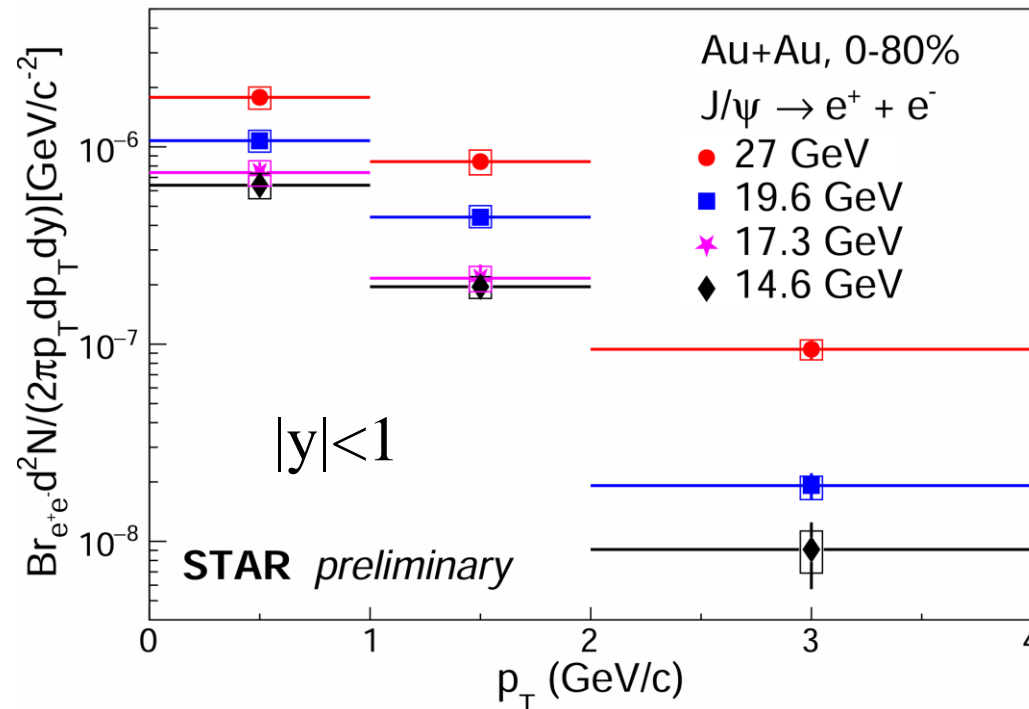


Acceptance correction and ϵ_{TPC} are getting from embedding sample

Inclusive J/ψ Invariant Yields



$$R_{AA} = \frac{\sigma_{\text{inel}}}{\langle N_{\text{coll}} \rangle} \frac{d^2 N_{AA}/dydp_T}{d^2 \sigma_{pp}/dydp_T}$$



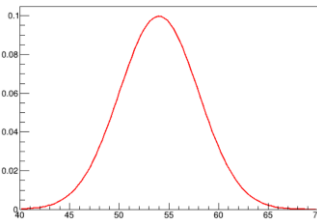
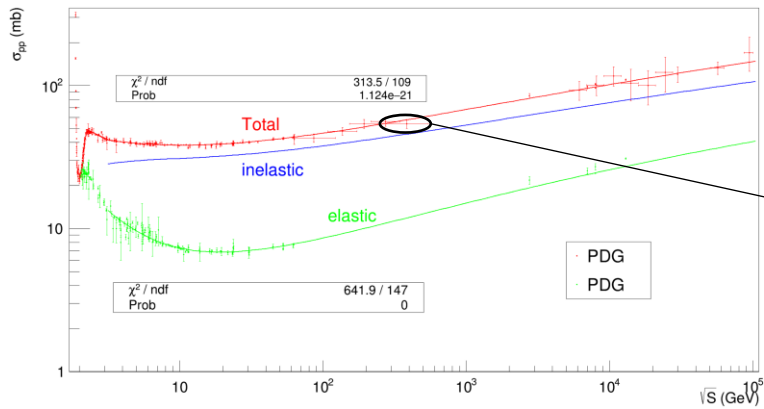
Inclusive J/ψ invariant yields as a function of p_T at mid-rapidity ($|y| < 1$) in Au+Au collisions at $\sqrt{s_{NN}} = 14.6, 17.3, 19.6, 27$ GeV

pp Inelastic Cross Section

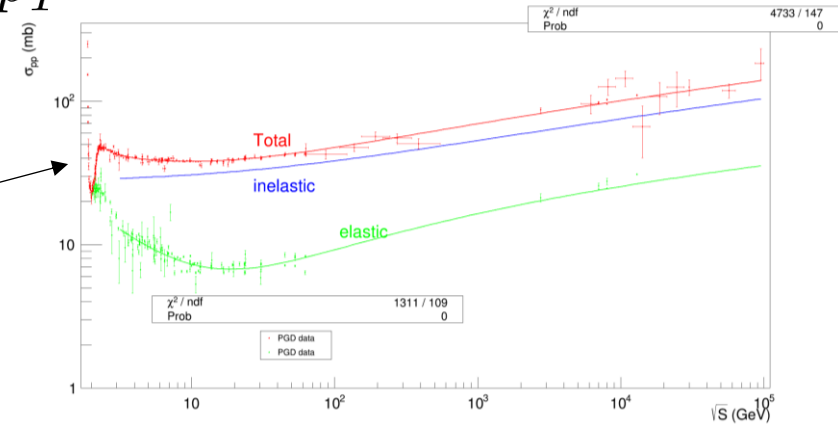


$$R_{AA} = \frac{\sigma_{\text{inel}}}{\langle N_{\text{coll}} \rangle} \frac{d^2 N_{AA} / dy dp_T}{d^2 \sigma_{pp} / dy dp_T}$$

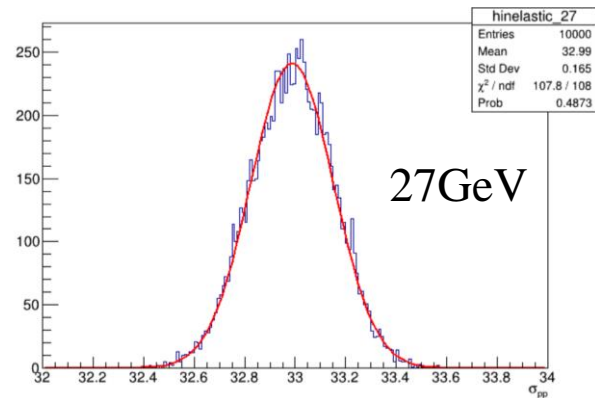
$$\sigma_{\text{inelastic}} = \sigma_{\text{total}} - \sigma_{\text{elastic}}$$



Smearing each point



Data from PDG (Particle Data Group) :
<https://pdg.lbl.gov/2022/hadronic-xsections/>



$\sqrt{S_{NN}}$ (GeV)	$\sigma_{\text{inelastic}}$ (mb)	Error(mb)
200	43.40	0.77
27	32.99	0.16
19.6	32.08	0.14
17.3	31.78	0.13
14.6	31.42	0.13
11.5	30.99	0.12
9.2	30.65	0.13

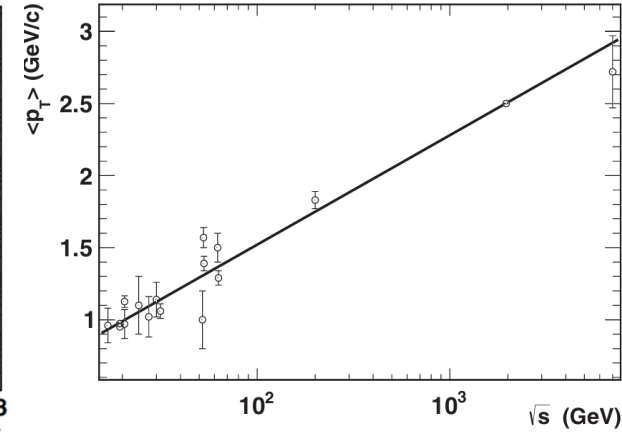
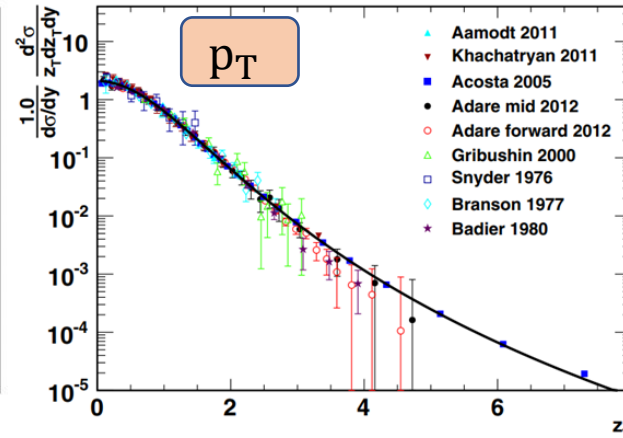
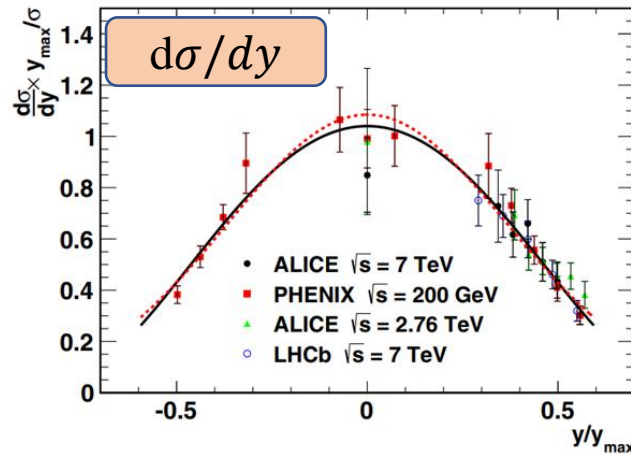
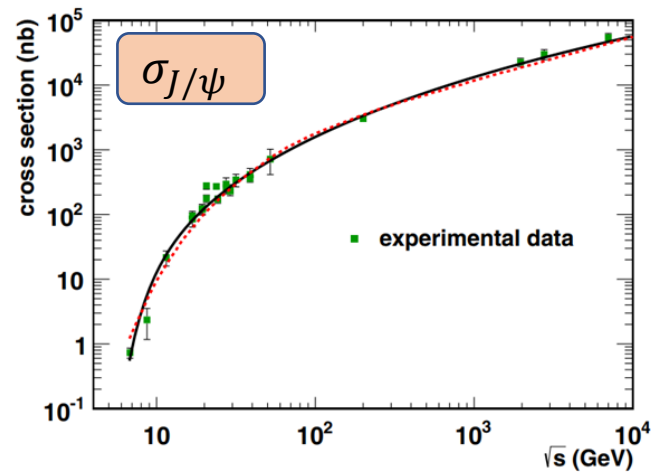
p+p Baseline



$$R_{AA} = \frac{\sigma_{\text{inel}}}{\langle N_{\text{coll}} \rangle} \frac{d^2 N_{AA} / dy dp_T}{d^2 \sigma_{pp} / dy dp_T}$$

- p+p baselines at $\sqrt{s_{NN}} = 14.6, 17.3, 19.6,$ and 27 GeV are extracted from phenomenological interpolations

W. Zha, et al., Phys. Rev. C 93 (2016) 024919.



$$\sigma = \alpha \times \sigma_{CEM}$$

α : scale factor

σ_{CEM} : σ from color evaporation model

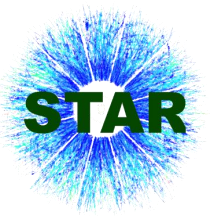
$$\frac{1}{\sigma} \frac{d\sigma}{d(y/y_{max})} = a e^{-\frac{1}{2} \left(\frac{y/y_{max}}{b} \right)^2}$$

where $y_{max} = \ln\left(\frac{\sqrt{s}}{m_{J/\psi}}\right)$

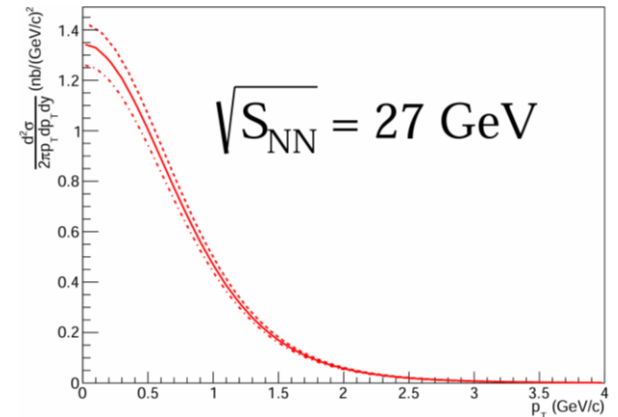
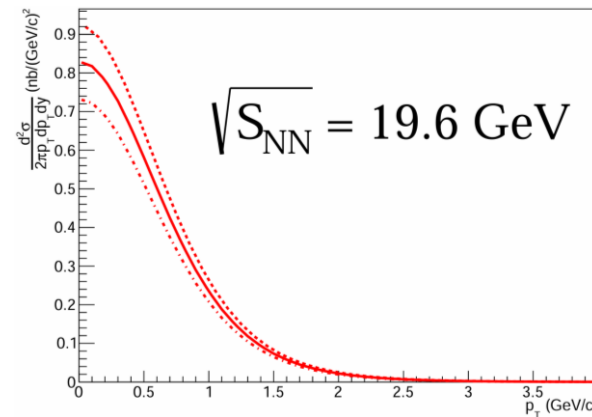
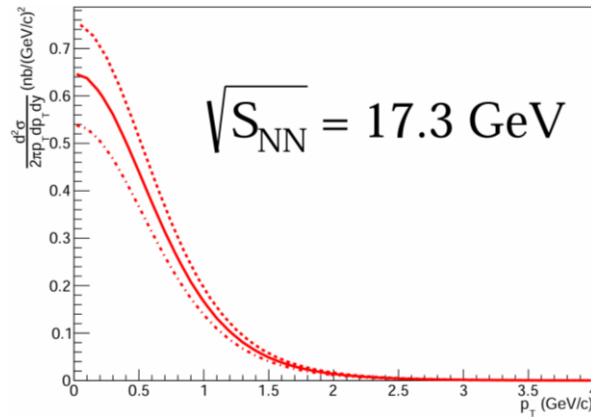
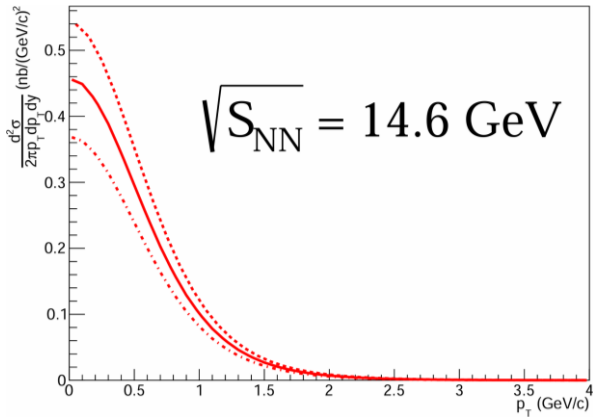
$$\frac{1}{d\sigma/dy} \frac{d^2\sigma}{z_T dz_T dy} = a \times \frac{1}{(1+b^2 z_T^2)^n}$$

where $z_T = p_T / \langle p_T \rangle$

p+p Baseline



$$R_{AA} = \frac{\sigma_{\text{inel}}}{\langle N_{\text{coll}} \rangle} \frac{d^2 N_{AA} / dy dp_T}{d^2 \sigma_{pp} / dy dp_T}$$



- The p_T dependence of deduced J/ψ differential cross section at midrapidity in p+p collisions at $\sqrt{s_{NN}} = 14.6, 17.3, 19.6, 27 \text{ GeV}$

- The systematic uncertainty arises from fitting world-wide data:

$\sqrt{s_{NN}} = 14.6 \text{ GeV}$	19.2 %
$\sqrt{s_{NN}} = 17.3 \text{ GeV}$	16.7%
$\sqrt{s_{NN}} = 19.6 \text{ GeV}$	11.7 %
$\sqrt{s_{NN}} = 27 \text{ GeV}$	6.1 %

Systematic Uncertainty



➤ Systematic uncertainty from J/ψ yield measurements

Source:

Track Quality Cuts

- nHitsFit
- nHitsDedx
- Dca (cm)

Signal Extraction

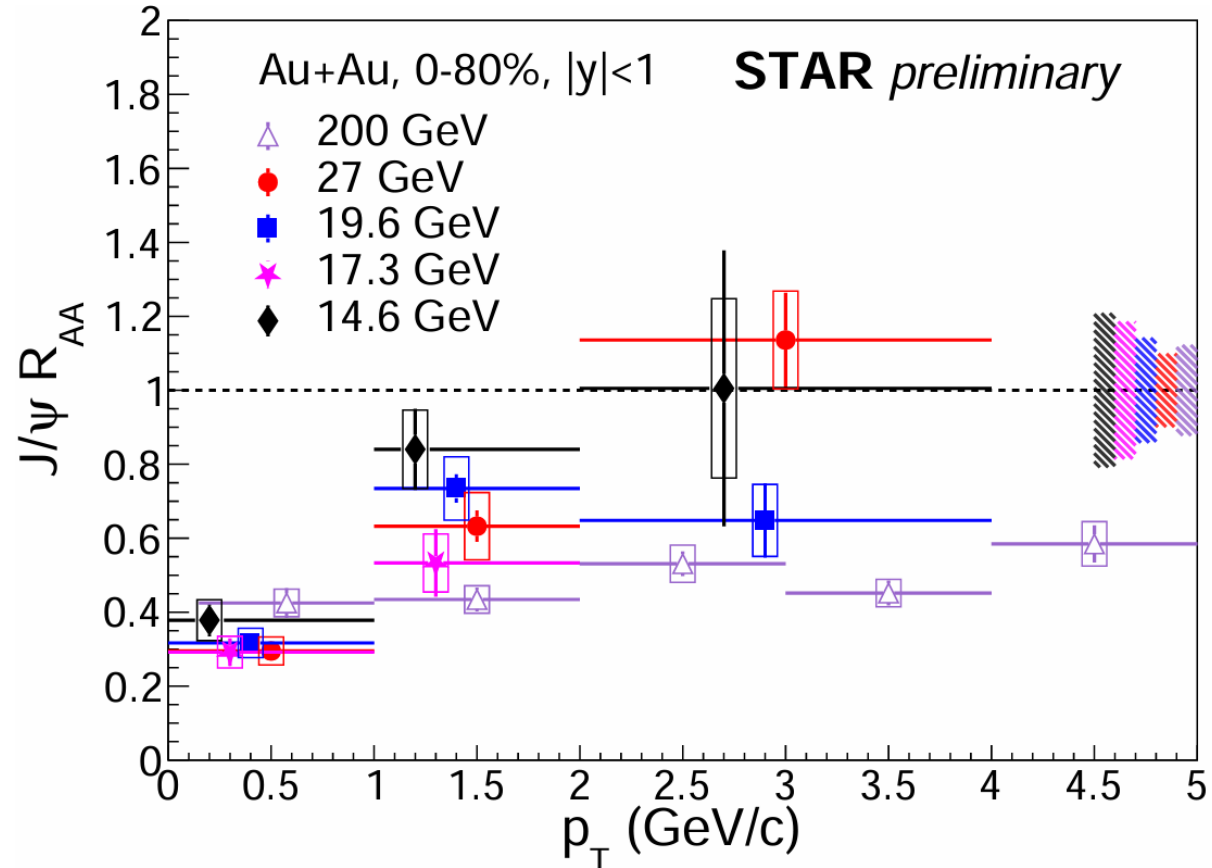
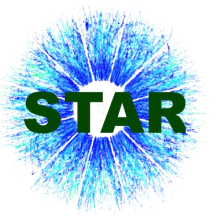
- J/ψ templates
- Fitting range
- Residual background function
- Combinatorial background function
- Bin Width

Electron Identification Cuts

- $n\sigma_e$ efficiency
- $1/\beta$ efficiency
- TOF Matching efficiency

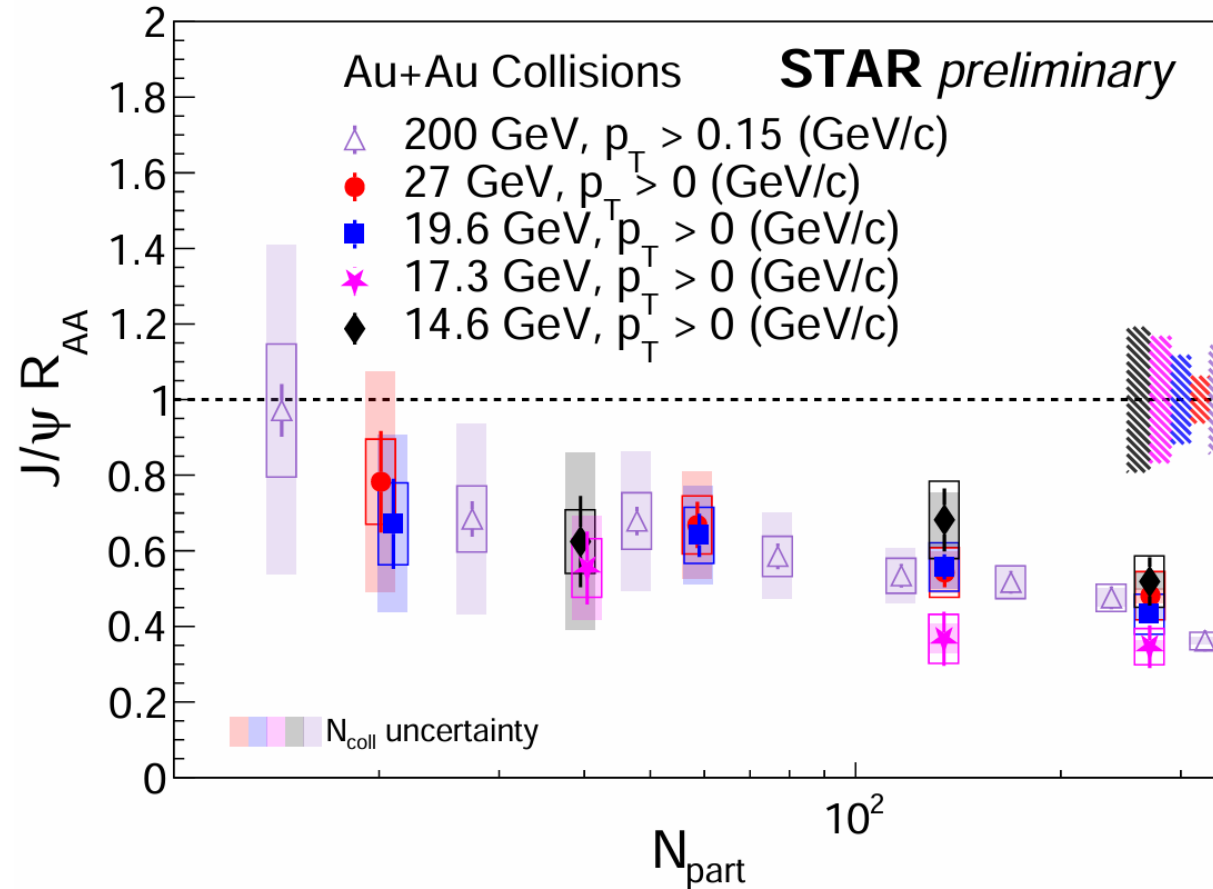
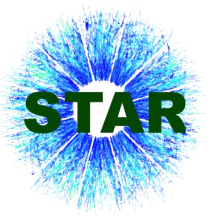
Analyzed bin	27 GeV	19.6 GeV	17.3 GeV	14.6 GeV
0-80 %	12.4 %	11.2 %	12.8 %	13.2 %
0-20 %	13.2 %	12.3 %	13.8 %	13.1 %
20-40 %	12.1 %	11.5 %	17.7 %	15.0 %
40-60 %	11.5 %	11.6 %	13.9%	13.5 %
60-80 %	14.4 %	16.1 %		
0-1 GeV/c	12.8 %	12.5 %	14.7 %	14.6 %
1-2 GeV/c	14.4 %	11.6 %	14.7 %	12.7 %
2-4 GeV/c	11.6 %	15.0 %	-	24.1 %

p_T Dependence of Inclusive J/ψ R_{AA}



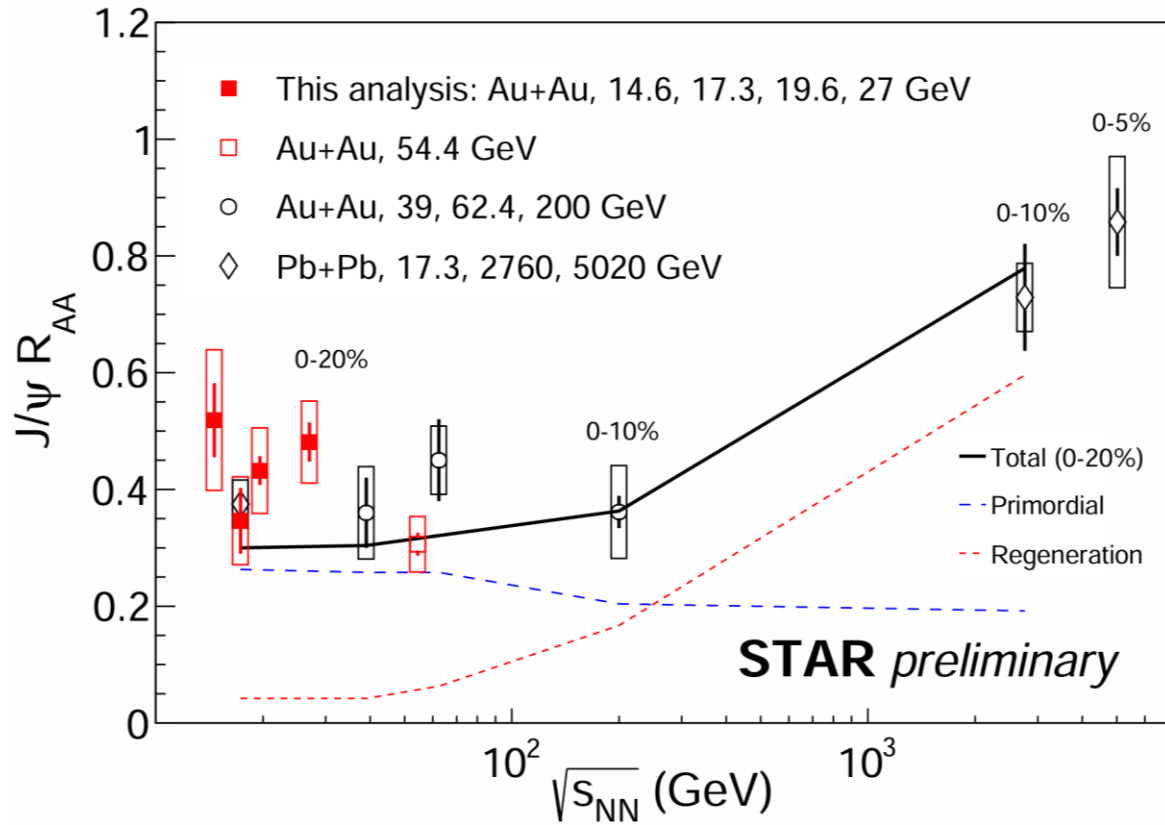
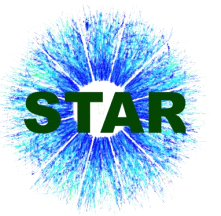
- Low p_T suppression, R_{AA} increases with p_T for $\sqrt{s_{NN}} = 14.6, 17.3, 19.6$ and 27 GeV
- No significant p_T dependence at 200 GeV

Centrality Dependence of Inclusive J/ψ R_{AA}



- Hint of decreasing trend as a function of centrality
- R_{AA} shows no significant energy dependence at RHIC for similar $\langle N_{part} \rangle$

Energy Dependence of Inclusive J/ψ R_{AA}



- Data at $\sqrt{s_{NN}} = 14.6, 17.3, 19.6$ and 27 GeV follow the trend
- **No significant energy dependence of $J/\psi R_{AA}$ in central collisions is observed within uncertainties up to 200 GeV**
- The J/ψ suppression in the LHC energy region is weaker
 - Regeneration dominates at LHC energies
- The transport model qualitatively describes the observed energy dependence

X. Zhao, R. Rapp, *Phys. Rev. C* 82 (2010) 064905 (private communication).
L. Kluberg, *Eur. Phys. J. C* 43 (2005) 145.
NA50 Collaboration, *Phys. Lett. B* 477 (2000) 28.

ALICE Collaboration, *Phys. Lett. B* 734 (2014) 314
STAR Collaboration, *Phys. Lett. B* 771 (2017) 13-20
STAR Collaboration, *Phys. Lett. B* 797 (2019) 134917
ALICE Collaboration, *Nucl. Phys. A* 1005 (2021) 121769

- Significant suppression of J/ψ productions in RHIC BES-II are observed
 - Hint of decreasing with centrality and increasing with p_T for $J/\psi R_{AA}$ at low energies
 - No significant collision energy dependence of $J/\psi R_{AA}$ at RHIC
 - Stronger suppression at RHIC than LHC, indicate smaller regeneration effect at RHIC
- Interplay of dissociation, regeneration and cold nuclear matter effects

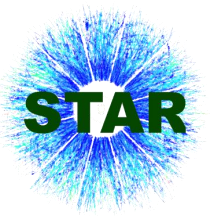


Thank you



Back up

Efficiency and Acceptance Corrections

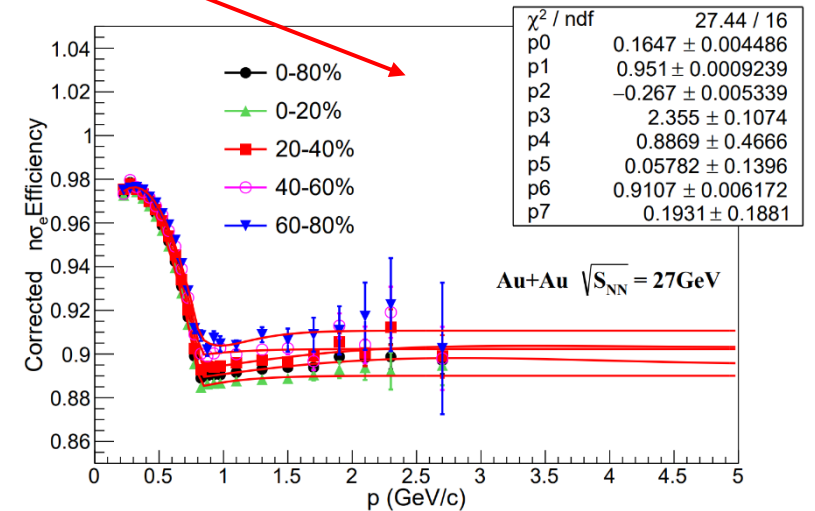
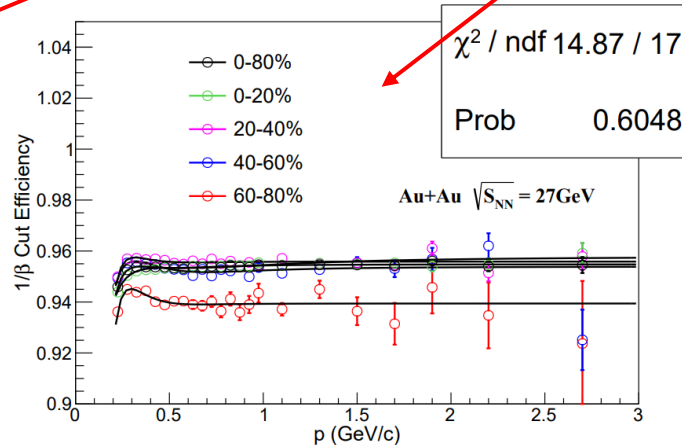
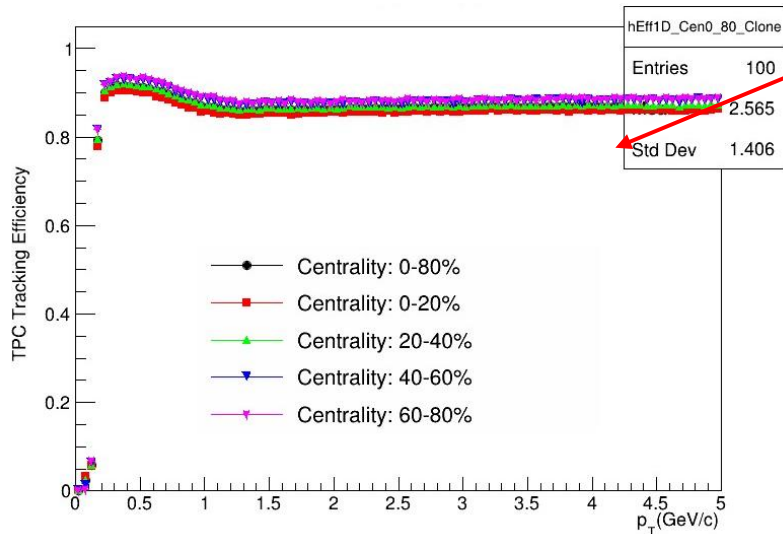


$$R_{AA} = \frac{\sigma_{\text{inel}}}{\langle N_{\text{coll}} \rangle} \frac{d^2 N_{AA} / dy dp_T}{d^2 \sigma_{pp} / dy dp_T}$$

$$N_{AA} = \frac{N_{J/\psi \rightarrow e^+e^-}}{A \times \epsilon \times N_{\text{event}}}$$

$$\epsilon = \epsilon_{\text{electron}} \times \epsilon_{\text{positron}}$$

$$\epsilon_{\text{electron}} = \epsilon_{\text{positron}} = \epsilon_{\text{TPC}} \times \epsilon_{\text{eID}} \times \epsilon_{\text{TOF}}$$

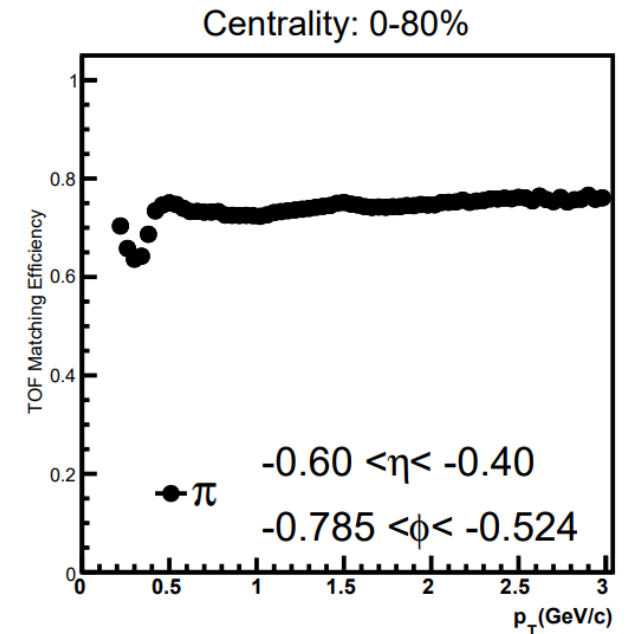
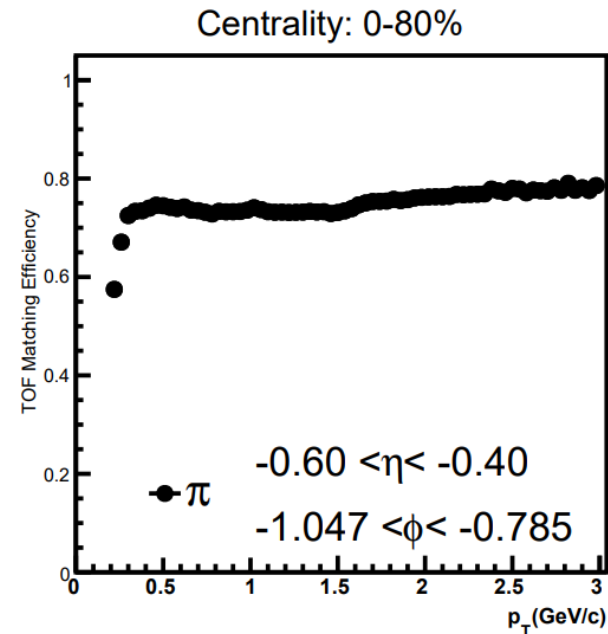
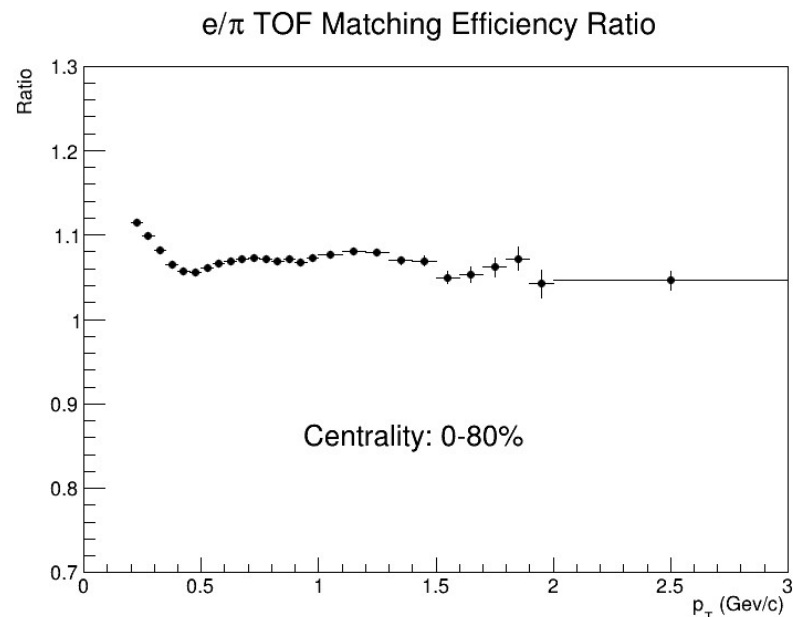


Efficiency and Acceptance Corrections



- TOF Matching efficiency has p_T η Φ dependence

$$\epsilon_{\text{electron}} = \epsilon_{\text{positron}} = \epsilon_{\text{TPC}} \times \epsilon_{\text{eID}} \times \epsilon_{\text{TOF(3D)}}$$

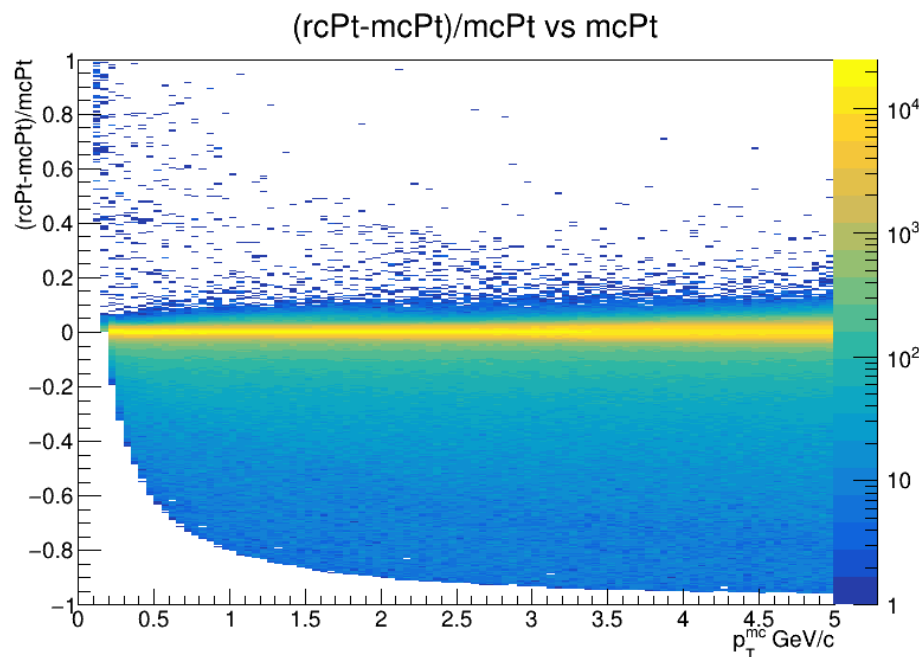


$$\frac{\text{Electron TOF Matching Efficiency (3D)}}{\text{Pion TOF Matching Efficiency (3D)}} = \frac{\text{Electron TOF matching efficiency (1D)}}{\text{Pion TOF matching efficiency (1D)}}$$

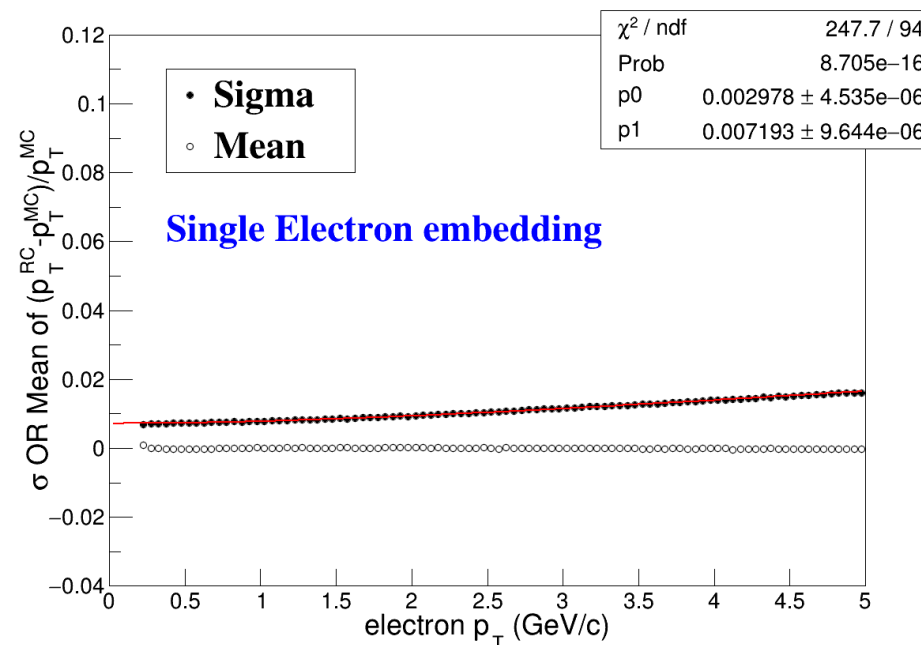
Additional Momentum Smearing (27GeV example)



$$p_T^{\text{smear}} = p_{T, \text{ True}} + \Delta p_T \times \frac{\sqrt{(a')^2 P_T^2 + b^2}}{\sigma^{\text{embed}}(p_{T, \text{ True}})} \longrightarrow \text{additional momentum smearing factor}$$

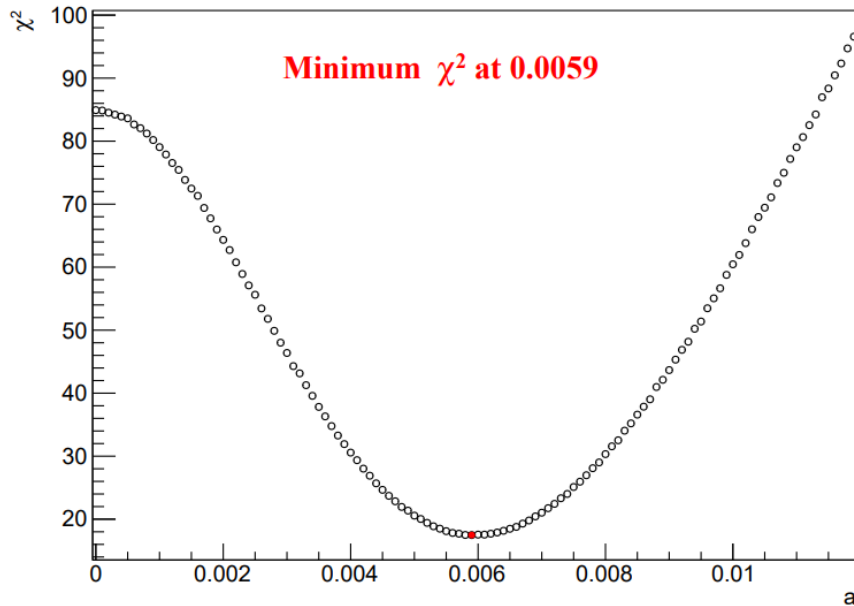


Embedding ID:20192501

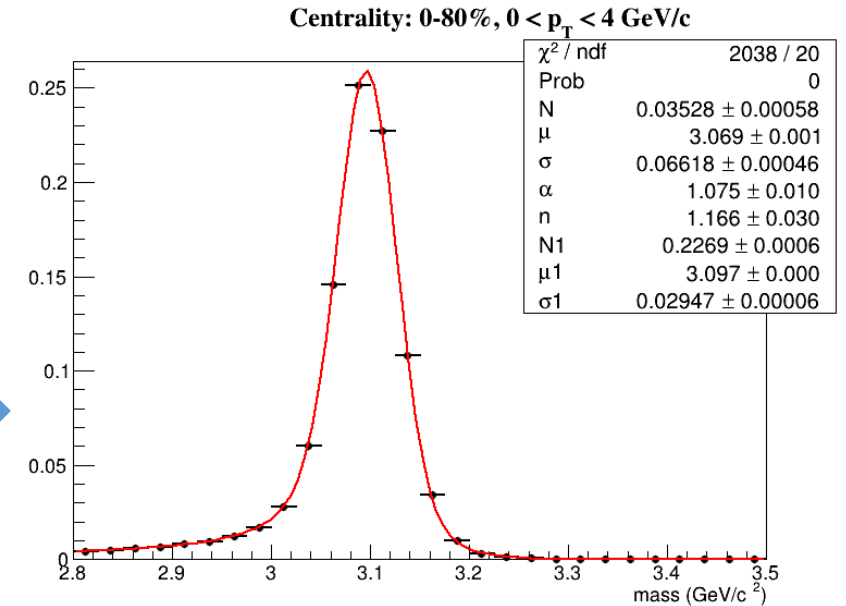


$$\sigma^{\text{embed}} = \sqrt{a^2 P_T^2 + b^2}$$

Addiction Momentum Smearing (27GeV example)



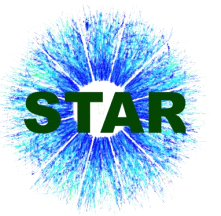
The J/ψ templates from ToyMC with additional momentum smearing based on best a .



scan a' \longrightarrow get J/ψ σ from ToyMC

\longrightarrow compare with data, a' value with minimum χ^2 is the best a' value

Systematic Uncertainty at Au + Au 27 GeV



Analyzed bin	Signal Extraction	Track	$N\sigma_e$	$1/\beta$	TOF Matching	Total
0-80%	2.1 %	10.3 %	5.5 %	3.3 %	0.8 %	12.4 %
0-20%	2.7 %	10.3 %	7.6 %	2.1 %	0.5 %	13.2 %
20-40%	1.8 %	10.6 %	4.6 %	3.1 %	0.2 %	12.1 %
40-60%	1.8 %	10.2 %	3.7 %	2.8 %	1.9 %	11.5 %
60-80%	3.8 %	10.5 %	8.4 %	3.7 %	0.06 %	14.4 %
0-1GeV/c	2.8 %	10.8 %	5.2 %	3.3%	1.1 %	12.8 %
1-2GeV/c	2.1 %	10.6 %	8.9 %	3.3%	0.8 %	14.4 %
2-4GeV/c	2.5 %	10.4 %	3.2%	3.2%	0.06 %	11.6 %

Consistency Checks

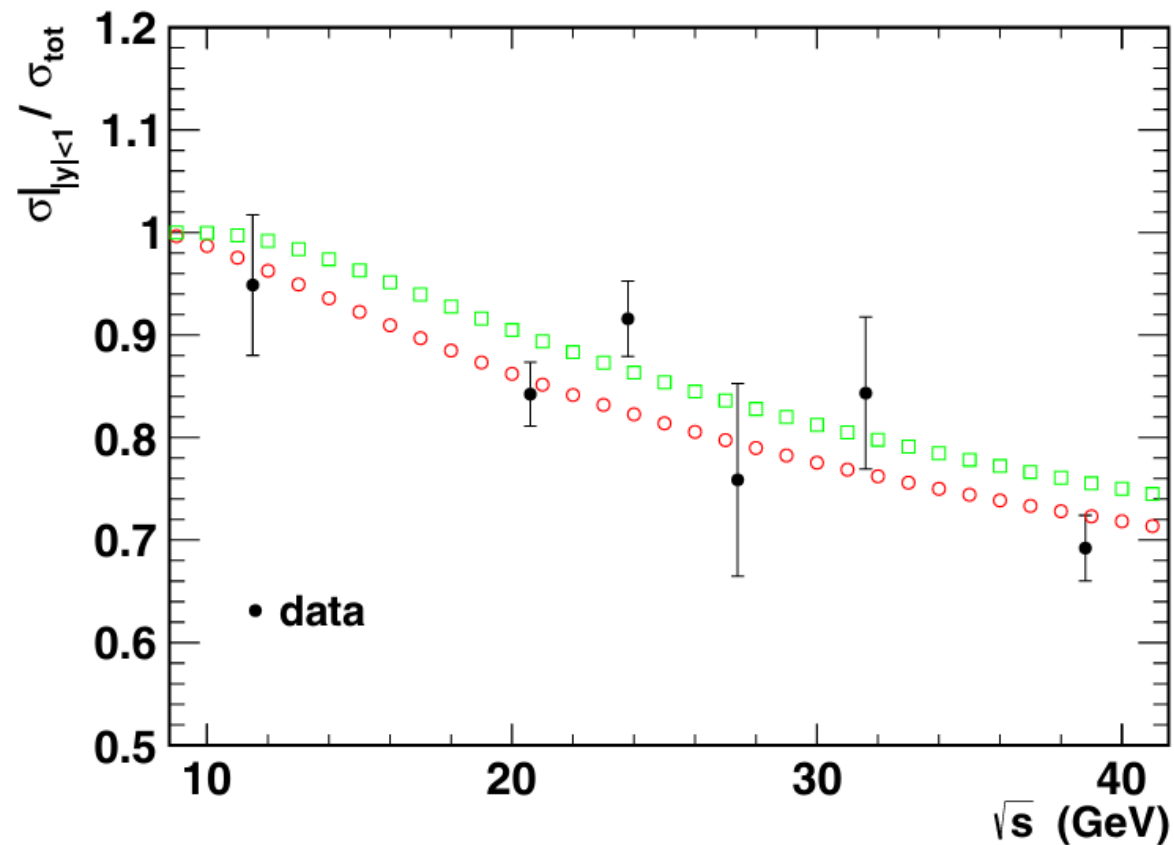


FIG. 7. The ratios of J/ψ $\sigma_{|y|<1.0}$ to σ_{tot} as a function of cms energy [16–18,30,32–34,37,50]. The open circle and the open square are the estimations using the function fit of Eqs. (6) and (7) in Fig. 4, respectively.



Systematic Uncertainty

➤ Systematic uncertainty from J/ψ yield measurements

Source:

Track quality cuts

- nHitsFit
- nHitsDedx
- Dca (cm)

Signal extraction

- J/ψ templates
- Fitting range
- Residual background function form
- Combinatorial background function form
- Bin Width

Electron Identification cuts

- $n\sigma_e$ efficiency
- $1/\beta$ efficiency
- TOF Matching efficiency

Analyzed bin	27 GeV	19.6 GeV	17.3 GeV	14.6 GeV
0-80%	12.4 %	11.2 %	12.8 %	13.2 %
0-20%	13.2 %	12.3 %	13.8 %	13.1 %
20-40%	12.1 %	11.5 %	17.7 %	15.0 %
40-60%	11.5 %	11.6 %	13.9%	13.5 %
60-80%	14.4 %	16.1 %		
0-1GeV/c	12.8 %	12.5 %	14.7 %	14.6 %
1-2GeV/c	14.4 %	11.6 %	14.7 %	12.7 %
2-4GeV/c	11.6 %	15.0 %	-	24.1 %

pp Inelastic Cross Section



- The parameters:
 - Glauber model inputs:
 - Collision system: Au+Au
 - Energy: 27 GeV
 - Radius of Au: $R = 6.38$ fm
 - Skin depth: $d = 0.535$ fm
 - Sigma(NN) = 33 mb
 - Separation of two nucleons: $ds = 0.9$ fm

$\sqrt{s_{NN}}$ (GeV)	$\sigma_{\text{inelastic}}$ (mb)	Error(mb)
200	43.40	0.77
27	32.99	0.16
19.6	32.08	0.14
17.3	31.78	0.13
14.6	31.42	0.13
11.5	30.99	0.12
9.2	30.65	0.13

The input sets in Glauber model	
Mode	Au + Au
Energy	17.3 GeV
Events	10^6
Radius of Au	$R = 6.38$ fm
Skin Depth	$d = 0.535$ fm
Inelastic NN cross section	$\sigma_{NN} = 31.8$ mb

The parameters (Glauber model inputs)	
Collision system	Au + Au
Energy	14.6 GeV
Radius of Au	$R = 6.38$ fm
Skin depth	$d = 0.535$ fm
Sigma(NN)	32 mb